sustainability

MDPI

Article

Increasing the Sustainability of the Stabilization/Solidification of Potentially Toxic Elements Contained in Tailings from an Active Mine Using a Modified Lime Mortar

Jesús F. González-Sánchez [1], Georgina Fernández-Villagómez [1], Alan Ulises Loredo Jasso [2], José M. Fernández [3], Íñigo Navarro-Blasco [3] and José I. Alvarez [3,*]

[1] Faculty of Engineering, National Autonomous University of Mexico, Coyoacan 04510, Mexico City, Mexico; fidel129@comunidad.unam.mx (J.F.G.-S.)
[2] Laboratory of Molecular Environmental Geochemistry (IGL-LANGEM), National Autonomous University of Mexico, Coyoacan 04510, Mexico City, Mexico; uloredo@geologia.unam.mx
[3] MATCH Research Group, Chemistry Department, School of Sciences, University of Navarra, 31008 Pamplona, Navarra, Spain; jmfdez@unav.es (J.M.F.); inavarro@unav.es (Í.N.-B.)
* Correspondence: jalvarez@unav.es

Abstract: The use of a modified lime mortar as a binder for the stabilization/solidification of mine tailings presents a promising and sustainable solution for immobilizing potentially toxic elements found in these waste materials compared to cement mortars. The effectiveness of this modified lime mortar in avoiding the mobility of toxic elements, namely lead (Pb) and arsenic (As), in mine tailings has been thus studied. Encapsulating matrices of 1:1 and 2:1 tailings waste/air lime ratios were prepared. Due to the content of potentially pozzolanic compounds in the mine tailings, mainly some silicate phases, 1:1 matrices showed better mechanical strength than 2:1 samples, ascribed to a more intense pozzolanic reaction. SEM observations identified needle-shaped C-S-H structures. The hardened materials showed good endurance against freeze–thaw cycles. The semi-dynamic tank test demonstrated the effective encapsulation of the toxic components due to the use of lime mortars, yielding values of released Pb and As below the detection limit in all instances. Considering the cost-effectiveness, widespread availability, and ease of use, the use of modified lime mortar for the treatment of mine tailings can be recommended to mitigate the environmental impacts of mining activities.

Keywords: solidification/stabilization; mine tailings; lime mortar; encapsulation; arsenic; lead; pozzolanic reaction

Citation: González-Sánchez, J.F.; Fernández-Villagómez, G.; Loredo Jasso, A.U.; Fernández, J.M.; Navarro-Blasco, Í.; Alvarez, J.I. Increasing the Sustainability of the Stabilization/Solidification of Potentially Toxic Elements Contained in Tailings from an Active Mine Using a Modified Lime Mortar. *Sustainability* **2024**, *16*, 2320. https://doi.org/10.3390/su16062320

Academic Editor: Syed Minhaj Saleem Kazmi

Received: 18 January 2024
Revised: 29 February 2024
Accepted: 7 March 2024
Published: 11 March 2024

1. Introduction

Mining in Mexico continues to be one of the main economic activities [1,2]. Toxic substances, along with a significant amount of energy, are used in the mining process, and they alter the sites from which precious metals such as gold and silver are extracted [3,4]. Waste generated from crushed rocks and minerals used to remove the desired metal [2,5,6] further contributes to the environmental impact. Large quantities of stones are required to obtain a few grams of precious metal. The waste produced during the extraction process, known as tailings, typically contains harmful elements such as lead, cadmium, arsenic, and mercury. Due to the presence of these elements, the waste becomes toxic to living organisms and significantly contributes to aquifer and food chain contamination [4–7]. In Mexico, the Nahuatl word "jales" is used, which means fine sand and accurately describes the physical form of these residues [8,9]. The tailings are disposed of in open-air tailings dams, initially in the form of sludge. However, due to climatic conditions and the passage of time, they begin to dry out to the point of forming mounds of very fine

sand that can easily be dispersed by the wind [10]. Furthermore, due to weathering, some tailings dams form leachates and acid drainage when their chemical composition includes sulfur minerals, such as pyrites [5,10,11]. This leads to another environmental problem: groundwater aquifers may be polluted, and dissolved potentially toxic elements can be carried and absorbed by the surrounding biota or even contaminate adjacent farmland and enter the food chain, causing health issues [1,12,13].

Typically, the solidification/stabilization process involves blending solid waste with binding agents such as cement, asphalt, and others, aiming to attain favorable physical characteristics while simultaneously trapping hazardous components within the solidified material [14]. One of the proposed treatments for this type of waste is solidification/stabilization, which has been investigated by different authors using Portland cement as the main binder [15–20]. Through the utilization of Portland cement, various contaminants become encapsulated within an interlocked mineral structure. As cement hydration progresses, the release of these contaminants decreases, which is attributed to the solidified contaminated material possessing a diminished surface area of contact with the leaching media and reduced permeability [20,21]. Portland cement can effectively encapsulate potentially toxic elements, but it is not a sustainable material and can be costly. In addition to Portland cement, different binders are available, such as gypsum or lime [22]. Another alternative as a binder in stabilization/solidification is the use of geopolymers, which offer an interesting alternative with faster setting times, potentially higher strength and durability, and reduced environmental impact compared to Portland cement [3,23]. However, the use of lime mortar to treat this type of waste has not been sufficiently researched. The advantage of using lime as a binder is that it emits less CO_2 and can capture it through carbonation during hardening. Its production requires less energy consumption, making it cheaper. It is also an abundant natural material whose manufacturing process compared to cement turns out to be less complicated and more sustainable [24–26]. Currently, lime is used by literally thousands of waste generators in the United States and elsewhere for solidification/stabilization treatment in a broad sense [14,17,22]. Initially, it neutralized acidic wastewater and precipitated metals before discharge. Still, it was found that the encapsulating systems could meet leaching test standards simply by using an excessive amount of lime. Lime has also been independently employed to stabilize or solidify waste containing high levels of organic components such as oil or tar, making it hydrophobic [15,22,27].

On the other hand, it has been observed that lime-based solidification/stabilization, in general, is not as effective in reducing metal leaching as cement-based systems [14,19,27,28]. To support this statement, the very high pH that typically results from lime-based systems and the large porosity both in the matrix and in the encapsulating components as well as the different chemical compositions of the binding matrix in comparison with cement-bearing systems should be mentioned [22]. However, by improving pozzolanic processes, a modified lime-based mortar can incorporate metals such as lead into the silica matrix as effectively as cement [29–31]. In the current work, the rationale is that the composition of the tailings, containing high levels of silicates [32–34], might aid in the hydraulic properties of lime mortar, thus resulting in increased compressive strength and weather resistance [8,35,36].

This research aims to assess the immobilization of potentially toxic elements present in previously characterized mine tailings using the stabilization/solidification technique, with the help of a sustainable modified lime mortar as a binder. Additionally, this study aims to determine the resulting mixture's chemical, physical, and mechanical properties. This approach is proposed as a more sustainable treatment to mitigate the health and environmental damages caused by this waste.

The current study utilizes mine tailings previously examined by González et al. in 2023 [32], with Pb and As as the primary potentially toxic elements. These tailings are incorporated as aggregates in a mixture with a modified lime mortar binder to facilitate the solidification/stabilization treatment process. Initially, a sufficient mixture is prepared

to create cylindrical monoliths using PVC molds, which are then cured in a chamber with controlled humidity and temperature for 28 days. Subsequently, various physicochemical tests, including compression resistance and tank testing, are performed to verify their compatibility and assess the effectiveness of the solidification/stabilization treatment with this modified mortar. This approach presents an alternative treatment for mine tailings dams, aiming to prevent their migration from the dam to the surrounding population and avoid the health issues outlined in González et al.'s 2023 study.

2. Materials and Methods

2.1. Materials

To evaluate the stabilization/solidification treatment, twenty different mixes were prepared to create the monoliths under study, using mining tailings samples reported in the study by Gonzalez et al., 2023 [32]. Table 1 summarizes some properties of these samples [32], with the dam as an aggregate, modified lime mortar as a binder, and water. The binder used was a modified lime mortar named C5 lime concentrate supplied by Nanocal S.A, C.V (Mexico City, Mexico). According to the information provided by the supplier, the lime mortar is composed of air lime type CL90, and its composition includes marmoline as an aggregate with particle size 100 mesh (147 microns), diatomite and microsilica as pozzolanic agents, starch and cellulose as thickeners, sodium oleate as a water repellent, and a polyacrylic fiber. This modified lime mortar with ca. 40 wt. % of air lime was prepared by mixing the dry powder with 30 wt. % of mixing water.

Table 1. Summary of some physicochemical properties of the mine tailings samples (analyzed by González et al. [32]).

Number Sampling Point [33]	Characteristics						
			Mineralogical Compositions of Tailings According to FTIR-ATR Results				
	pH	H *	Functional Groups	Silicates		Carbonates	Arsenates
				Olivines	Feldspars		
1	6.1	6.6	$Si_3O_8^{4-}$ CO_3^{2-}	-	Orthoclase ($KAlSi_3O_8$) Microcline ($KAlSi_3O_8$) Oligoclase ($Ca_{0.1–0.3}Na_{0.7–0.9}AlSi_3O_8$) Albite ($NaAlSi_3O_8$) Andesine ($Ca_{0.3–0.5}Na_{0.5–0.7}AlSi_3O_8$)	Smithsonite ($ZnCO_3$) Magnesite ($MgCO_3$) Gaylussite ($Na_2Ca(CO_3)_25H_2O$)	-
2	7.1	11.6					
3	8.1	18.5					
4	7.1	8.1					
5	7.0	13.8					
6	7.0	3.0	SiO_4^{3-} AsO_4^{3-}	Andradite ($Ca_3Fe_2(SiO_4)_3$)		-	Adamite ($Zn_2(AsO_4)(OH)$) Berzelite ($(Ca;Na)_3(Mg;Mn)_2(AsO_4)_3$)
7	7.1	1.7	$Si_3O_8^{4-}$ CO_3^{2-}	-	Orthoclase ($KAlSi_3O_8$) Microcline ($KAlSi_3O_8$) Oligoclase ($Ca_{0.1–0.3}Na_{0.7–0.9}AlSi_3O_8$) Albite($NaAlSi_3O_8$) Andesine($Ca_{0.3–0.5}Na_{0.5–0.7}AlSi_3O_8$)	Smithsonite ($ZnCO_3$) Calcite ($CaCO_3$) Magnesite ($MgCO_3$) Gaylussite ($Na_2Ca(CO_3)_25H_2O$)	-
8	7.1	3.1					
9	7.1	8.7					
10	8.1	11.8					

* H: humidity.

2.2. Preparation of Samples

Mixes were prepared in accordance with the Mexican standard NMX C159 ONNCE-2016 [37]. Samples were prepared according to Table 2. All materials (mortar, tailings, and water) were mixed for 2 min in a low-speed Hobart mixer in compliance with EN 196–1 (European Committee for Standardization, 2018) [38]. Once the fresh mixture was ready, it was poured into PVC tube molds with a height of 5 cm and a diameter of 2.5 cm, resulting in 6 monoliths per mixture (3 of them for leaching tests to guarantee the representativeness of the results). These monoliths were then placed in the curing chamber at a constant temperature of 25 °C and 60% RH. Experimental units were de-molded 24 h after their creation and left in the chamber for 28 days in the aforementioned conditions. The amount of mixing water was adjusted until the fresh mixes had a settlement diameter of 165 mm in the flow table test, following EN 1015–3 [39].

Therefore, the name of each monolith is identified by the tailings point used for its fabrication and the tailings/binder ratio. The specimens were prepared by employing weight ratios of 1:1 and 2:1 for tailings/binder. For instance, the monolith made with tailings from point one, using a 1:1 ratio, is named 1 (1:1). The first digit corresponds to the sampling point of the mine tailings. The ratio in parentheses corresponds to the mine tailings/lime ratio (Table 1).

Additionally, a mixture of the modified C5 lime mortar with water was prepared as a control group.

Table 2. Materials for the production of monoliths, as well as the proportions used.

Sample	Mining Tailings Sampling Point [33]	Weight Ratio (Mine Tailings/Lime Mortar)	Mass of Mine Tailings (g)	C5 Concentrate Lime (Modified Lime Mortar) (g)	% Water *
Control	-	-	0	900	30
1 (1:1)	1	1:1	450	450	30
1 (2:1)		2:1	600	300	30
2 (1:1)	2	1:1	450	450	30
2 (2:1)		2:1	600	300	30
3 (1:1)	3	1:1	450	450	30
3 (2:1)		2:1	600	300	30
4 (1:1)	4	1:1	450	450	30
4 (2:1)		2:1	600	300	30
5 (1:1)	5	1:1	450	450	30
5 (2:1)		2:1	600	300	30
6 (1:1)	6	1:1	450	450	30
6 (2:1)		2:1	600	300	30
7 (1:1)	7	1:1	450	450	30
7 (2:1)		2:1	600	300	30
8 (1:1)	8	1:1	450	450	30
8 (2:1)		2:1	600	300	30
9 (1:1)	9	1:1	450	450	30
9 (2:1)		2:1	600	300	30
10 (1:1)	10	1:1	450	450	30
10 (2:1)		2:1	600	300	30

* Percentages with respect to the weight of modified lime mortar and mining tailings.

The most significant difference observed among the different monoliths is that, for example, monoliths 1 (1:1) and 1 (2:1) were made with mining tailings sample 1 taken from the top of the tailings dam and consisted mainly of this residue. In contrast, monoliths 10 (1:1) and 10 (2:1) were made with sample 10 taken from the base, where the mining

company had mixed some aggregates and even added a lime slurry onto the mining tailings, which was visually observed (Figure 1).

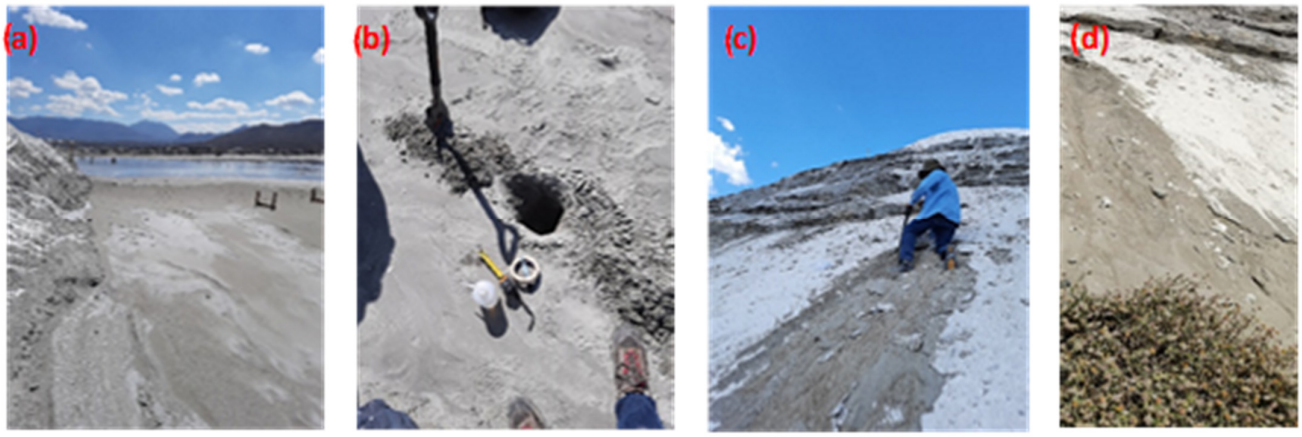

Figure 1. Different sampling areas of the tailings: (**a**) top of the tailings dam, (**b**) sampling point 1, (**c**) middle zone of the tailings dam, (**d**) base of the tailings dam, sampling point 10.

2.3. Characterization of the Samples

2.3.1. FTIR and X-ray Diffraction Studies

Compositions of the raw mine tailings and of the hardened specimens were carried out using a Thermo Scientific Nicolet iS10 FTIR spectrometer (Thermo Nicolet Corporation, Madison, WI, USA) with a GladiATR accessory featuring a diamond crystal. The sample was read with 64 scans at a resolution of 4 cm^{-1}, applying a background at the beginning of each analysis. To ensure the absence of moisture and CO_2, throughout this methodology, all samples were analyzed using N_2 (NUAP type) as the purge gas in the equipment.

XRD studies were conducted on powdered samples using a Bruker D8 Advance diffractometer (Bruker Scientific Instruments, Billerica, MA, USA) employing Cu Kα1 radiation, in a range spanning from 5° to 80° (2θ), with conditions of 1 s/step and a step size of 0.03°. A software Diffrac EVA (version 4.3.0.1, Bruker) was used to identify the presence of the crystalline phases comparing the diffraction peaks with the ICDD database. This software also provides a semi-quantitative estimation of the composition comparing the relative intensity of the main diffraction peak of each present compound.

2.3.2. Determination of Pore Size Distribution and Compressive Strength of Mortars

A Shimadzu compression machine with a capacity of 5000 kg was used to measure the compression strength of cylindrical mortars after 28 days of curing. The tests were conducted at a 5–50 kP s^{-1} breaking speed under ASTM C39 [40].

Porosity by mercury intrusion (MIP) was determined using a Micromeritics-AutoPoreIV-9500 (Micromeritics Instrument Corporation, Norcross, GA, USA) over a pressure range of 0.0015 to 207 MPa to establish the pore size distributions of hardened monoliths after the curing period.

2.3.3. Thermogravimetric Analysis (TGA)

The instrument used for thermogravimetric analysis was the SDT650 from TA Instruments, New Castle, DE, USA, and data evaluation was performed using TRIOS, also from TA Instruments. Approximately 10 mg samples were contained in 90 µL alumina pans. The heating program applied consisted of a heating ramp of 20 °C per minute, from 35 °C to 1000 °C, under a nitrogen atmosphere with a flow rate of 100 mL per minute. The weight loss percentages observed between 450 and 480 °C were linked to the dehydroxylation

process of uncarbonated portlandite, while the weight reductions at approximately 800–900 °C were assigned to the release of CO_2 from calcium carbonate.

2.3.4. Microstructural Analysis

Scanning electron microscopy (SEM) was employed with the COXEM EM-30N (COXEM Co., Ltd., Daejeon, Republic of Korea) electron microscope to examine the microstructure of the treated samples. Fractured surfaces of the samples were mounted on stubs with carbon tape and coated with gold using a COXEM SPT-20 Ion Coater (COXEM Co., Ltd., Daejeon, Republic of Korea). The coating process was carried out for 120 s at a current of 4 mA. Elemental analysis was performed using a Quantax Compact 30 Bruker EDS (Bruker Nano GmbH, Berlin, Germany) probe, and data management was carried out using the Esprit Compact software (version 2.3.1.1019, Bruker).

2.3.5. Durability

The strength of monoliths cured for 28 days was assessed under freezing–thawing conditions and sulfate attacks. The freezing resistance test involved immersing the samples in water for 24 h and subsequently freezing them at −10 °C for 24 h. For these experiments, a CARAVELL 521-102 freezer (Caravell Ltd., Buckingham, UK) was utilized.

The structural integrity of the samples was visually evaluated after each freezing–thawing cycle, following a previously reported criterion from 0 to 5 [41], which categorized the treated specimens as follows:

- 0. None: No observable changes in samples lacking any indications of decay;
- 1. Scarce: Samples displaying minor degradation, characterized by slight, brief, and superficial cracks on the surface;
- 2. Moderate: Modified samples exhibiting numerous deeper cracks;
- 3. Large: Highly transformed specimens with profound cracks and a certain level of expansion;
- 4. Very large: Samples undergoing severe deterioration, featuring deep cracks, partial loss of weight, and notable swelling;
- 5. Total: Samples wholly ruined, with only fragments remaining.

2.3.6. Leaching Tests

The mining tailings underwent the PECT test, a procedure established in the NOM-053-SEMARNAT-1993, [42] which allowed us to determine the leaching concentration of potentially toxic elements in waste material.

The leaching behavior of potentially toxic elements in mortars was assessed using a semi-dynamic tank test (norm EA NEN 7375) [43]. In this test, a complete sample was submerged in a leaching fluid composed of demineralized neutral pH water, and the leachate was periodically renewed. Thirty cylindrical test specimens measuring 50 mm × 25 mm were placed within sealable methacrylate tanks measuring 110 mm × 110 mm × 110 mm. These tanks were filled with 1 L of demineralized neutral pH water, serving as the leaching fluid. After the specified duration, all leachate was drained and filtered through a 0.45 μm pore size nylon membrane (Biomed Scientific, Biomed Scientific Limited). Conductivity and pH were measured using Corning pH-30-Conductivity Sensor equipment. Following draining and filtering, a fixed volume of 10 mL from each sample was preserved with sub-boiling nitric acid for subsequent analysis of the concentration of leached components. Subsequently, the tank was refilled with the same volume of water (1 L), and the procedure was repeated. Eluates were collected eight times (0.25, 1, 2.25, 4, 9, 16, 36, and 64 days) [16]. The concentration of leached As and Pb was determined using atomic absorption spectrometry (GBC AVANTA atomic absorption spectrophotometer equipped with a GBC HG 3000 peristaltic pump) (GBC Scientific Equipment Pty Ltd., Melbourne, Australia).

3. Results and Discussion

3.1. Lime Mortar Modified Characterization

In this mortar, portlandite was characterized by the typical band in this mineral at 3641.5 cm^{-1}, corresponding to the asymmetric stretching vibrations of the -OH group (see Figure S1 in the Supplementary Materials). This band is easily distinguished from the one generated by water or Si-OH interactions in silicates (~3400 cm^{-1}), allowing it to be uniquely assigned to this mineral phase. Based on the vibrations v1, v2, and v3 (1110, 872.7, and 1410.4 cm^{-1}, respectively), the presence of carbonates in the sample is confirmed, as these vibrations correspond to symmetric and asymmetric stretching of the CO_3^{2-} group. However, what explicitly defines the presence of calcium carbonate (calcite) is the typical band in this mineral observed at 711.5 cm^{-1} (v4, asymmetric stretching in-plane). Regarding silicates, various bands originating from them are observed, such as those at 1110 and 440 cm^{-1} (Si-O and O-Si-O vibrations, respectively). Regarding C-S-H phases, Zarzuela et al. (2020) report two characteristic bands, the first at ~960 cm^{-1} corresponding to the asymmetric stretching vibrations of Si-O in the SiO_4^{4-} group, and the second, a small band at ~810 cm−1, related to the symmetric vibration of the mentioned bond in the same SiO_4^{4-} [44]. Both bands are observed in this mortar, confirming their presence. In addition to the water band at ~3400 cm^{-1}, the presence of two other bands corresponding to vibrations in the H-O-H and -OH bonds (1651 and 1582 cm^{-1}, respectively) is also observed.

3.2. Effect of Mining Tailings Encapsulation on the Properties and Microstructure of the Mortars

Figure 2 shows an increase in the mechanical properties in the 1:1 mixes as compared with the plain lime mortar (control group) [45]. This fact can be ascribed to the presence of mine tailings that, due to their high content of silicates, can enhance pozzolanic reactions and consequently increase the C-S-H phases of the mortar [36,46]. As a consequence, the compressive strength of these specimens increased. As tailings have a very reduced particle size [32], there is increased contact of the binder in the specimens with high lime content (1:1), enhancing the chemical processes of C-S-H gel formation at their interface. According to the literature, this results in a strengthening of the bond between the binder and the aggregate, consequently leading to an improvement in strength results [47,48]. It can be seen that compressive strength values for (1:1) samples were generally above 4 MPa, with some specimens yielding near 8–10 MPa. The literature has reported values around 1–2 MPa for hydraulic lime mortars, around 4 MPa for hydraulic lime with 10 wt. % of additional metakaolin, and around 7 MPa for 20 wt. % of additional metakaolin [45]. The compressive strengths of the mortars prepared in the current study showed values above the previously published values, pointing to a resistant hardened matrix.

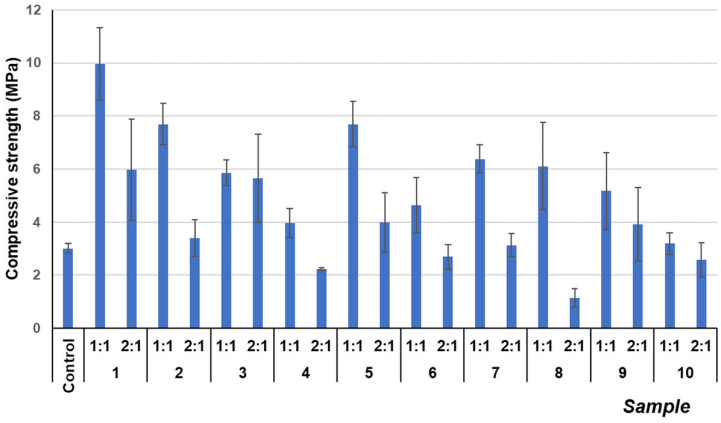

Figure 2. Compressive strength results of different mixes after 28 curing days.

However, samples with (2:1) ratios exhibited lower compressive strengths than those of (1:1) samples. In these specimens with large amounts of mine tailings, the relatively low amount of lime in the mortar fails to achieve a homogeneous mixture and to act as a binding phase, and thus, the formation of C-S-H phases declined, as shown in the FTIR spectra of the samples (Figure S2 of the Supplementary Materials). The signals corresponding to ca. 960 cm^{-1} (typical of the C-S-H phases) and corresponding to the asymmetric stretching vibrations of the Si-O in the SiO_4^{4-} are present in all the samples (see Figure S3 in the Supplementary Materials). The evidence of pozzolanic reactions included the control sample, which had air lime and pozzolanic agents in its composition. In general, a more marked band is observed in the (1:1) composition samples. TG analyses below will provide further confirmation of this performance.

The differences in strength values between the different sampling points of mine tailings 1 to 10 were ascribed to the variation in tailings composition. The mine tailings samples are highly heterogeneous and of different natures [32,49]. While point 1 has the largest percentage of residues with pozzolanic reactivity, point 10 has fewer active components and more inert aggregates and non-reactive sand granules (see Section 2.1). The different compositions of the mine tailings and their heterogeneity according to the sampling points account for the differences in mechanical strength.

To further investigate the differences in compressive strengths between the samples with mine tailings/lime ratios of 1:1 and 2:1, the porosity of the hardened specimens was measured (Figure 3). The porosity values showed, for example, a reduction in porosity of up to 21% (sample 9 (1:1)) and up to 28% (sample 3 (2:1)) compared with the control sample (Figure 3). This may be due to the density difference between the mining tailings and the lime mortar. Although specimens with 2:1 ratios have lower porosity than those with 1:1 ratios, they did not exhibit the highest compressive strengths. These 2:1 samples presented greater density in the monolithic structure than that of the 1:1 samples, due to the significantly higher density of the tailings (Figure 4). This confirms that the decrease in porosity is a consequence of the density and particle size of the mining tailings [8]. Nevertheless, if a mixture is more saturated with tailings, the binding matrix cannot aggregate and compact it properly, leading to a decrease in compressive strength.

In fact, the highest density was presented by sample 8 (2:1), which turned out to have one of the lowest compressive strengths and a notable difference with sample 8 (1:1). This more pronounced difference, in addition to the reasons mentioned for the lower amount of binding phase, is attributed, compared to the samples of points 9 and 10, to the presence of lime slurry poured by the mining company in the latter (see Section 2.2). In any case, the heterogeneity of the mine tailings themselves generated this variability between samples.

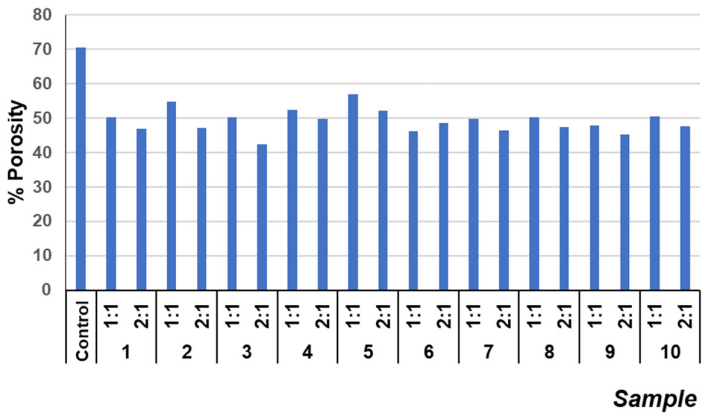

Figure 3. Porosity values of different mixes at 28 curing days.

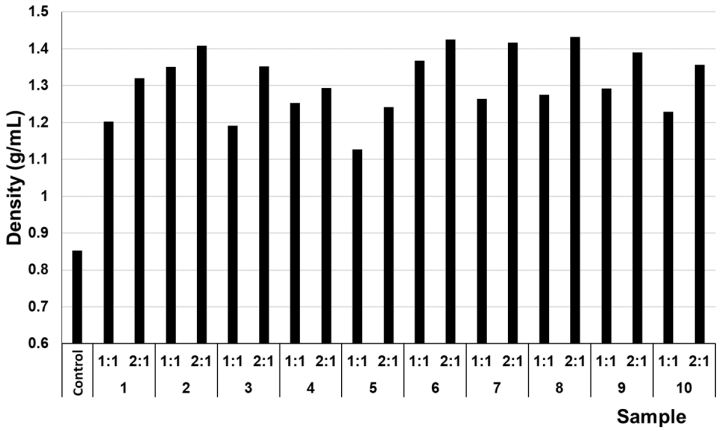

Figure 4. Densities of the different monoliths after 28 days of curing.

The mineralogical study of the hardened specimens revealed that they do not contain substantial amounts of pyrites or sulfate-bearing compounds. Therefore, the samples did not show a large formation of expansive components like ettringite. Detailed X-ray diffraction (XRD) analysis showed small amounts of pyrites and minimal quantities of newly formed ettringite (Figure 5). The samples with 1:1 ratios mainly presented calcite (around 70–75%), 1–5% of non-carbonated portlandite (that had not reacted to form calcium silicates), ca. 10% of microcline (a very abundant silicate in the encapsulated mine tailings), and minor amounts (below 5%) of components such as scawtite, biotite, ettringite (consistently below 3%), chalcopyrite, and telluride of lead, iron, and copper (Figure 5). Samples with 2:1 ratios showed a larger amount of unreacted original components of the mine tailings, but the differences regarding the major phases between the diverse sampling points were rather negligible.

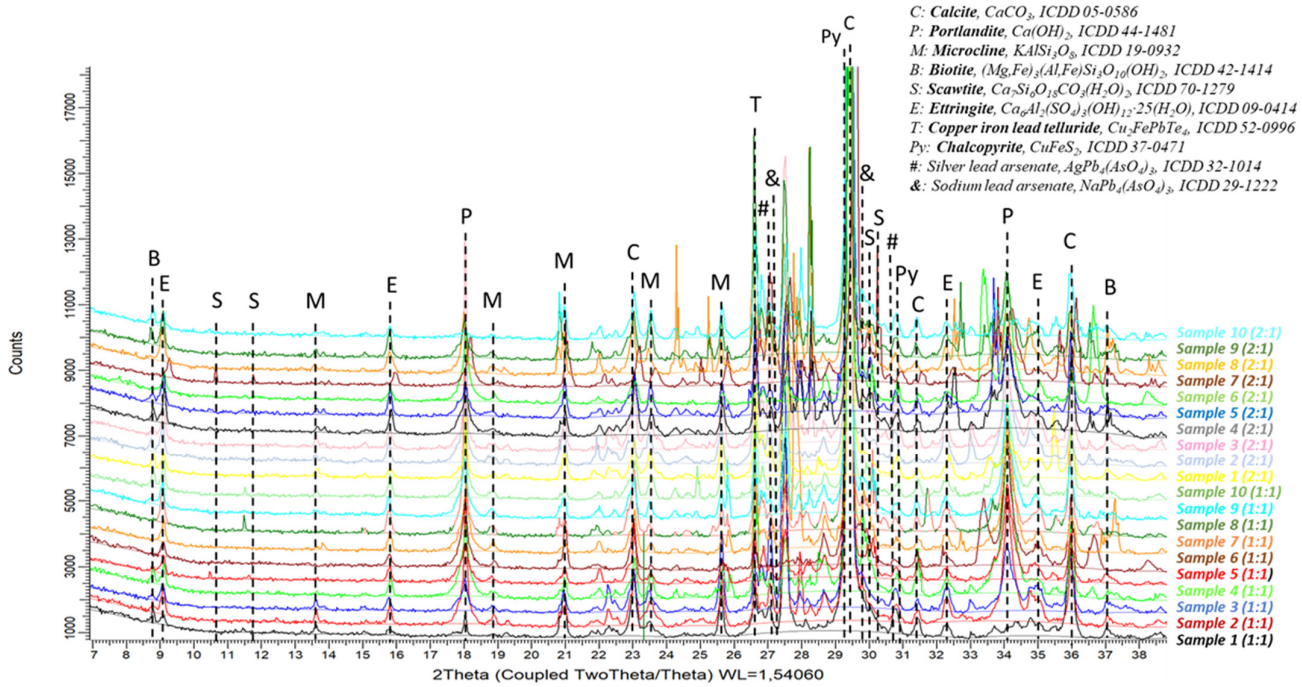

Figure 5. XRD profiles of the hardened samples.

No significant changes in the crystalline phases dependent on the tailings' sampling points were found in the XRD patterns, as shown, as an example, in Figure 5, where the similarity between the diffractograms of lime mortars with tailings encapsulated in the same ratios for the different sampling points can be seen.

The $CaCO_3/Ca(OH)_2$ ratio was determined through thermogravimetric analysis, which is directly proportional to the degree of carbonation in the mixes (Figure 6). The ratio of all samples containing mining tailings showed an increase compared to the control sample. This indicates the consumption of free $Ca(OH)_2$ due to the pozzolanic reaction. The control sample exhibited the highest $CaCO_3$ percentage (59.4%), but it showed a very low $CaCO_3/Ca(OH)_2$ ratio. This was because the control sample also presented the highest percentage of unreacted portlandite (22.7%) due to the absence of the pozzolanic reaction. As observed, doubling the amount of mining tailings in the monoliths (mixtures from 1 (2:1) to 6 (2:1)) reduced the $CaCO_3/Ca(OH)_2$ ratio because of the increase in the unreacted portlandite, confirming that increasing the amount of tailings in the mixes led to a decrease in the pozzolanic reaction due to the lower amount of the binding phase [32]. However, the ratios were higher than that of the control sample, and this was attributed to the silicates present in the mining tailings, which promoted the pozzolanic reaction, thus increasing the consumption of $Ca(OH)_2$.

The $CaCO_3/Ca(OH)_2$ ratio increased from samples 7 (2:1) to 10 (2:1). This was explained by the fact that, as detailed in the previous study, the mine tailings used in these samples contained carbonates, contributing to the rise in the ratio.

The complete analysis of the TG and DSC curves of the samples (Figure S4 in the Supplementary Materials) showed variability in the mine tailings and notable differences in the water content, which complicated the quantification of the hydrated fraction attributed to the phases C-S-H.

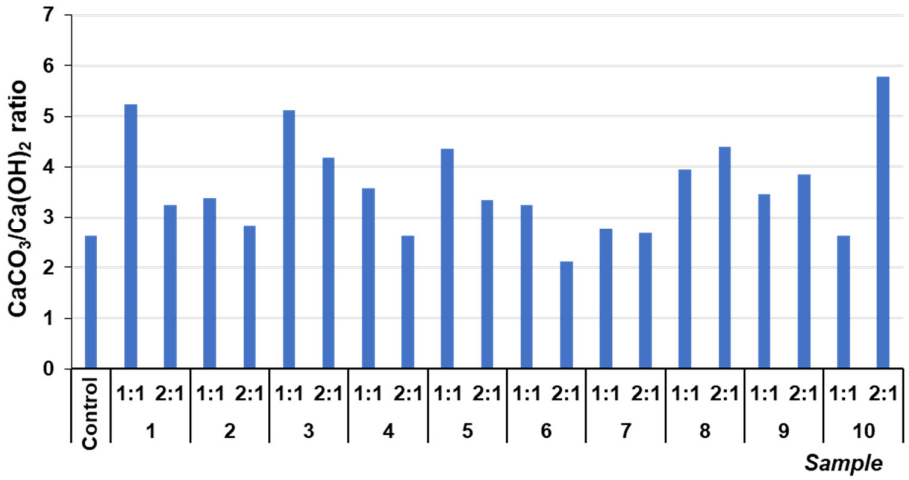

Figure 6. $CaCO_3/Ca(OH)_2$ ratio of different samples.

The microstructural analysis of the hardened specimens carried out by scanning electron microscopy confirmed the previous findings (Figure 7).

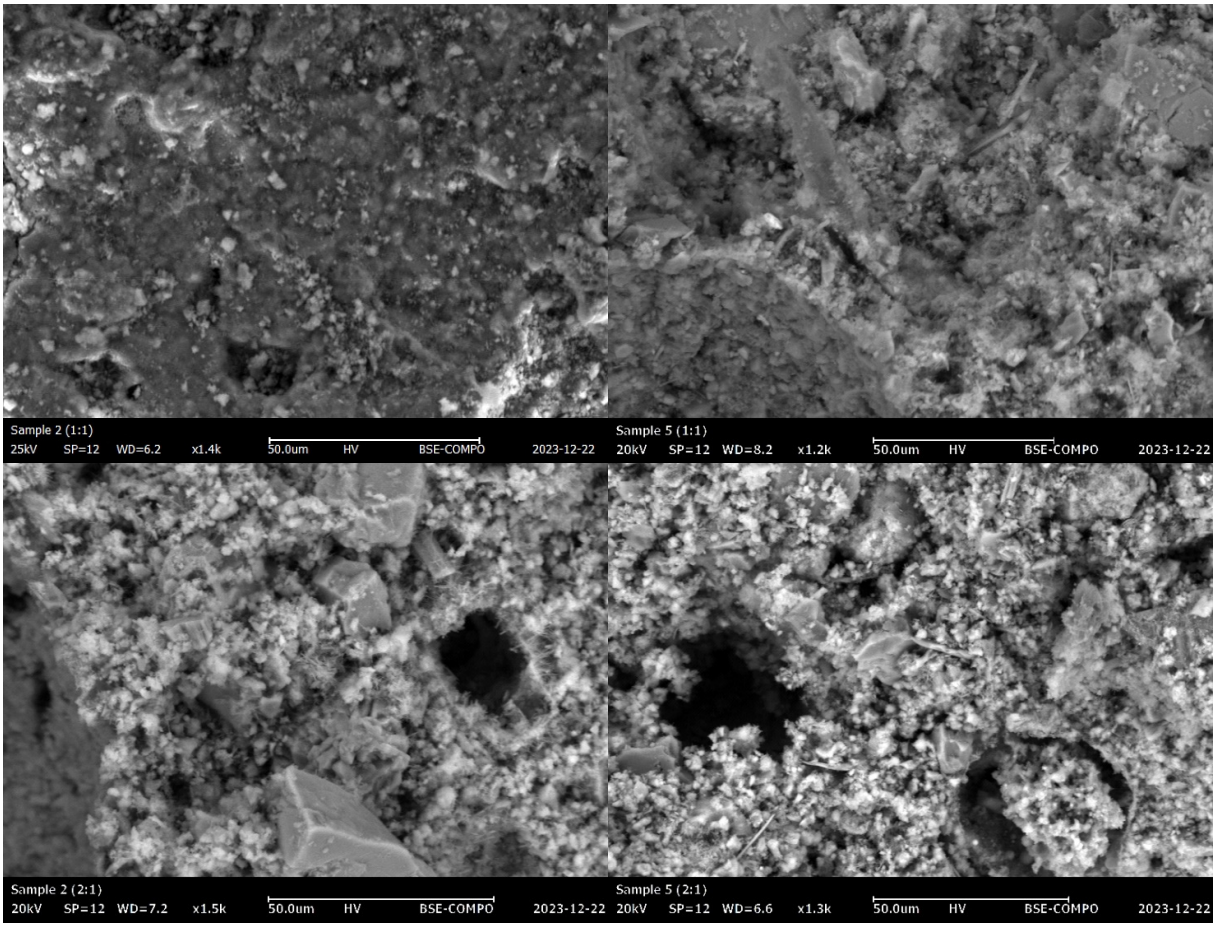

Figure 7. SEM micrographs of samples 2 (1:1), 2 (2:1)), 5 (1:1), and 5 (2:1) (top to bottom, left to right).

The micrographs show how the (1:1) samples had better compaction, which explains their higher compressive strengths. The more significant amount of binding phase (air lime) allowed better agglomeration of the tailings, forming a mechanically more robust system. On the other hand, the ratio of 2:1 generated a worse agglomeration of the tailings, with very visible macropores responsible for decreased mechanical resistance (Figure 7). Moreover, the granules and portions coming from the tailings were more clearly observed in the latter samples.

The pozzolanic reactivity of the tailings with the added lime is evidenced by the formation of abundant needle-shaped C-S-H structures, as shown in the following micrographs indicated with red arrows (Figure 8). According to the XRD results, ettringite was present, so it is likely that some of the needle-like structures were ettringite. The EDS results (Figures S5–S7 in the Supplementary Materials) showed that most of the needles do not present sulfur in their composition (and can be therefore associated with C-S-H phases, also because the presence of Ca, Si and O was demonstrated). However, a few of the needles presented sulfur in their composition (ascribed to the presence of a certain amount of ettringite, additionally identified by XRD) (Figure S3 in Supplementary Materials). It was also observed that the proportion of needle-shaped phases formed was higher in the samples with a (1:1) ratio.

In relation to the X-ray diffraction results previously discussed, the EDS examination of the samples confirmed the previous findings. Associations of Fe with S were found in the form of granules, establishing the presence of pyrites as determined by X-ray diffraction. Figure 9 shows a very noticeable central region composed of these pyrites. In addition, in Figure 9 and also in Figures 10 and 11, the Fe and S association was observed, and

Si, Al, and K were strongly combined with each other, responding to the abundant presence of microcline ($KAlSi_3O_8$), clearly determined by XRD. The presence of calcium silicates and silicoaluminates, not only as a result of the presence of compounds in the mine tailings but also as a result of the pozzolanic reaction, was also observed in these analyses. This association was evident in the spot analysis of the needle-shaped structures shown in Figure 9, as well as in the EDS results of spots of sample 10 (1:1) (Figure 12).

Other elements such as As and Pb appeared to be associated in certain spots (see Figure 11) in small amounts. These phases might be related to the presence of the original phases, especially arsenate (detected in the original tailing) with the substitution of some divalent cations by lead. To confirm this point, in various samples with high percentages of mine tailings, some weak X-ray diffraction peaks ascribed to the presence of arsenate compounds, at 29.7, 30.2, and 30.7° 2-theta, corresponding to a silver lead arsenate, and at 29.3, 30.82° 2-theta, corresponding to a sodium lead arsenate, were identified.

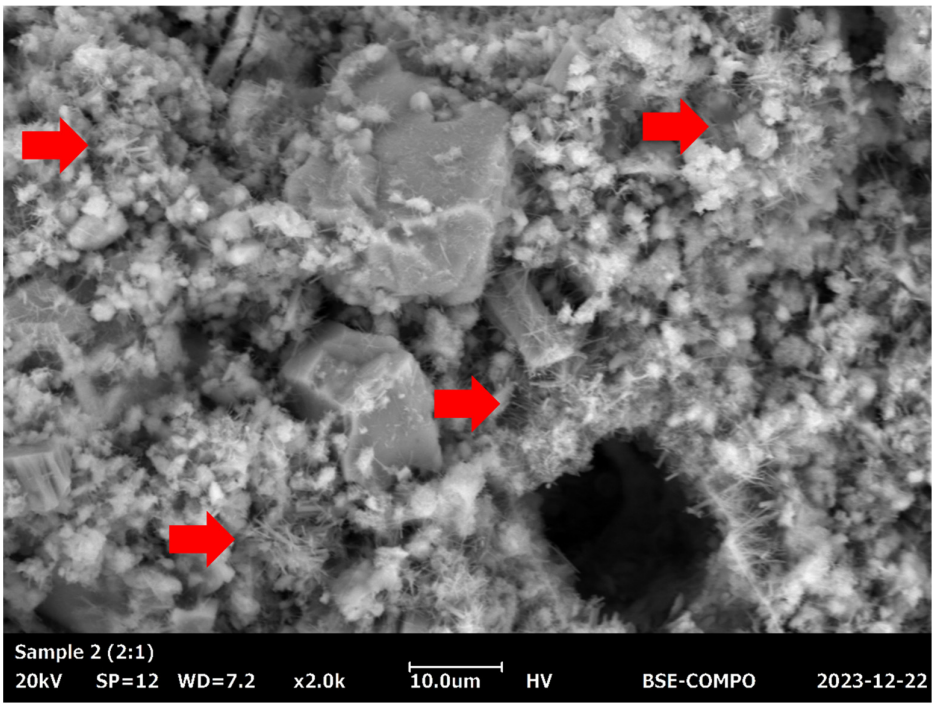

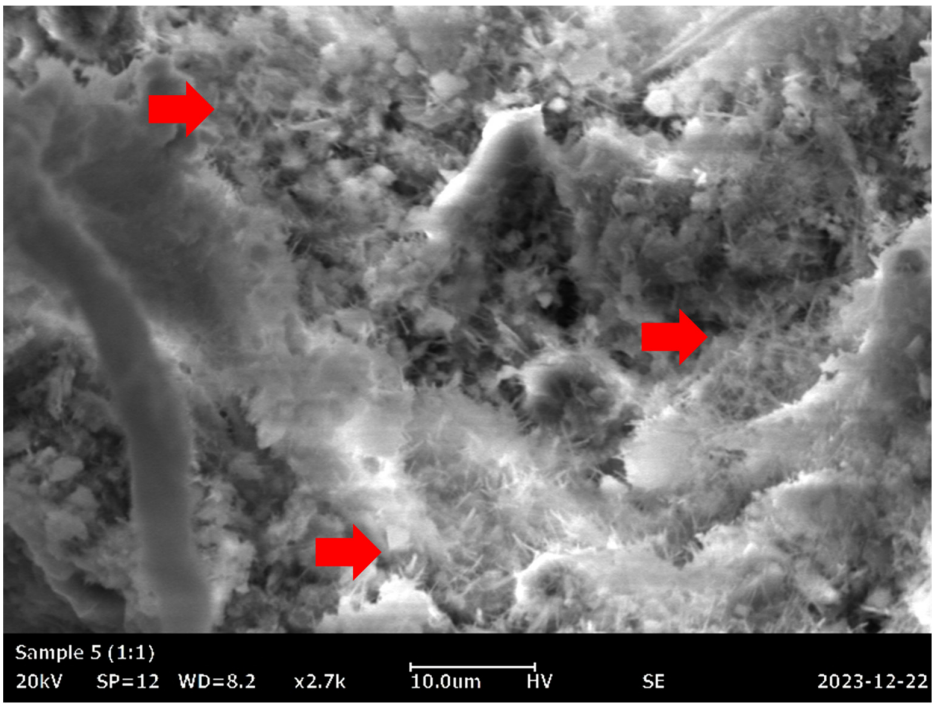

Figure 8. Needle-shaped C-S-H structures (red arrows) in samples 2 (2:1) (**top**) and 5 (1:1) (**bottom**).

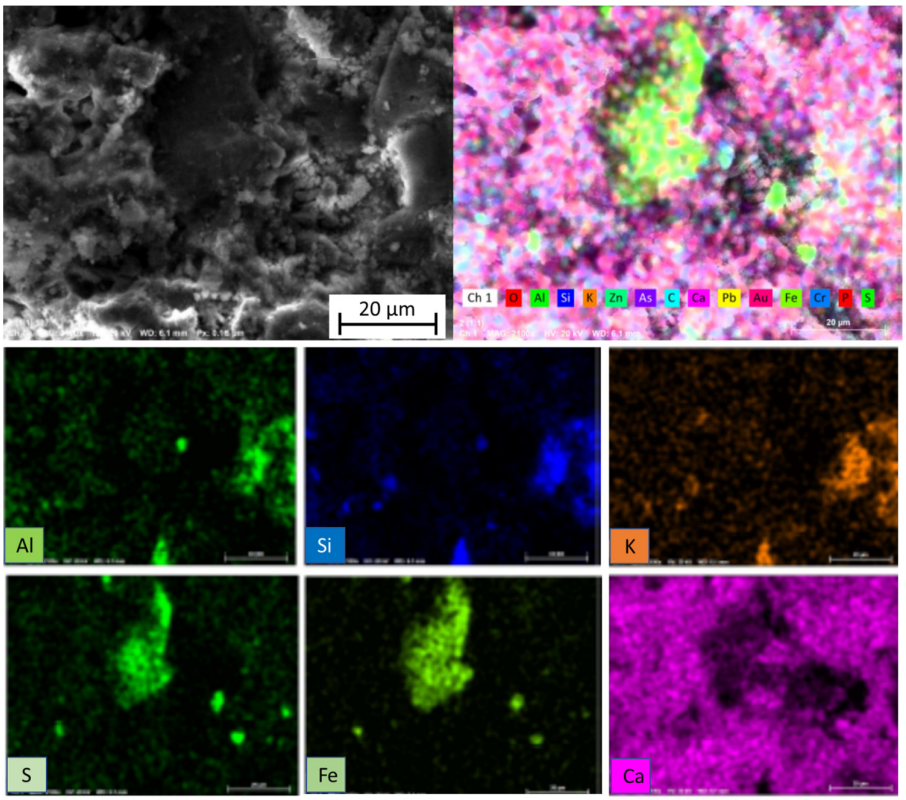

Figure 9. EDS element mapping of sample 2 (1:1).

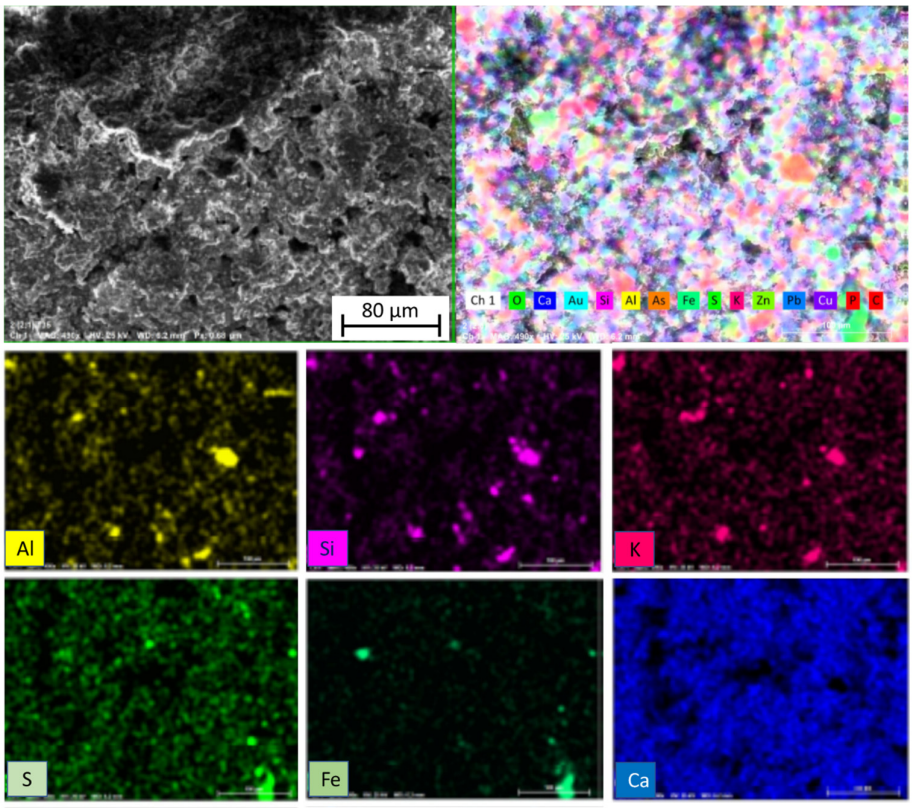

Figure 10. EDS element mapping of sample 2 (2:1).

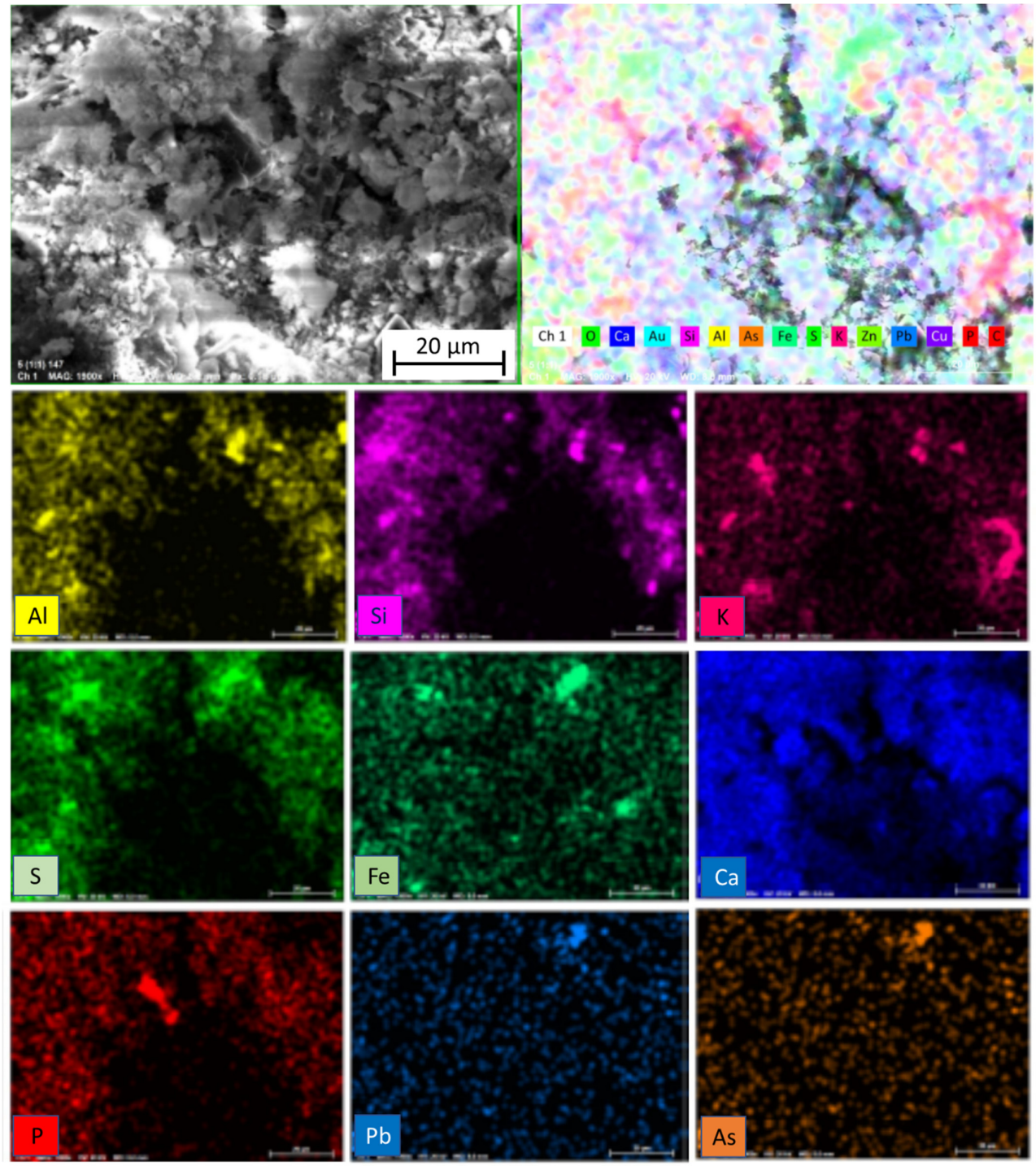

Figure 11. EDS element mapping of sample 5 (1:1).

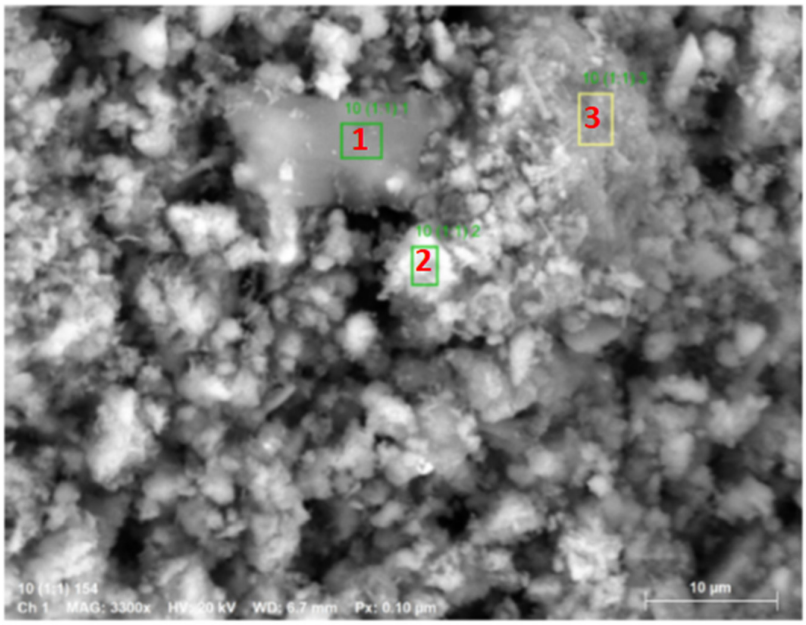

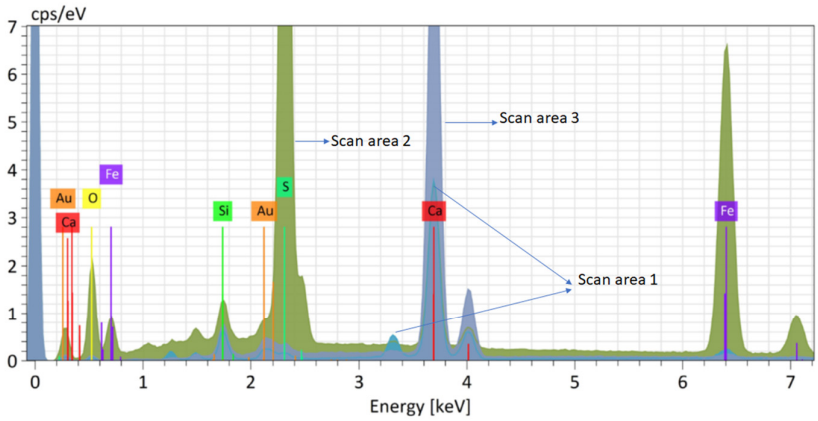

Normalized mass concentration [%]

Spectrum	C	O	Mg	Al	Si	S	K	Ca	Fe	Zn	Au
10 (1:1) 1	8.99	10.91	2.73	1.56	5.93	1.55	5.23	55.24	3.14		4.72
10 (1:1) 2	22.62	24.69		0.32	0.78	19.97	0.11	6.13	25.38	0.01	
10 (1:1) 3		13.28			4.98	1.27		73.25	1.03		6.20

Figure 12. EDS element composition results of spots of sample 10 (1:1).

3.3. Durability Experiments

The incorporation of mining tailings reduced the porosity of all assayed samples so that none of the samples suffered considerable damage up to 10 cycles (Figure 13). This demonstrates good compatibility in the setting of this residue with the modified lime mortar since no visually apparent structural damage occurred in any tested sample. They behaved similarly to the control sample and, in some cases, exhibited better resistance in this test, as seen in samples 6 to 10 in both proportions.

Under similar criteria, a detailed analysis of resistance to $MgSO_4$ sulfate attack is presented in Figure 14. During the initial six cycles, control samples showed no signs of

deterioration, while samples incorporating mining tailings exhibited mild effects from the fourth cycle onward. The degradation caused by sulfate attack was primarily explained through two mechanisms. On the one hand, the reaction of sulfate ions with portlandite and C-A-H led to the formation of voluminous and expansive compounds such as gypsum and ettringite, resulting in cracks and disruption of the hardened matrix [50]. This phenomenon suggests that the addition of mining tailings promoted the formation of these phases, as previously confirmed by the XRD results and by the SEM observations. On the other hand, the leaching of calcium from the C-S-H phases resulted in the loss of mechanical strength in the paste. According to the literature, the presence of Mg^{2+} ions (in the case of magnesium sulfate attack) causes decalcification of C-S-H through ionic substitution, increasing the degree of alteration [36,51].

The higher resistance to $MgSO_4$ attack could be associated with the presence of non-carbonated portlandite in all samples, preventing the formation of expansive sulfates, possibly due to the precipitation of magnesium hydroxide (brucite), and preventing the leaching of Ca from the C-S-H gel. As a result, an increase in the endurance of the samples was observed [51,52].

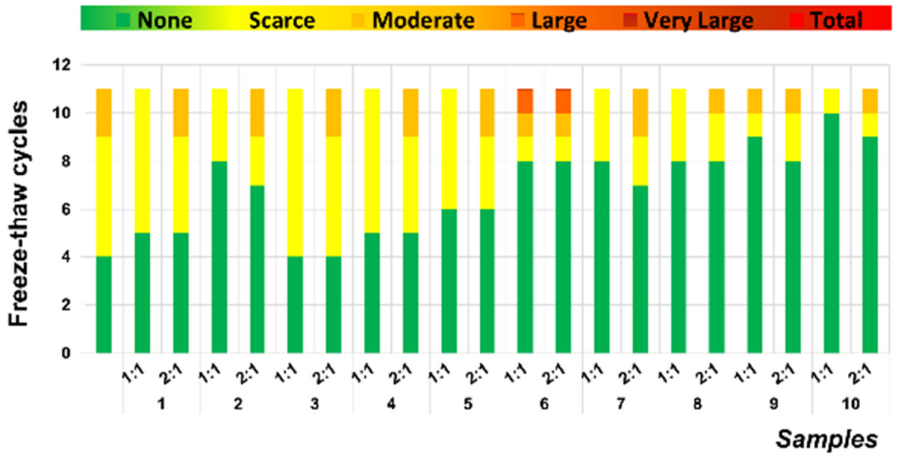

Figure 13. Degrees of alteration in samples following cycles of freeze–thaw.

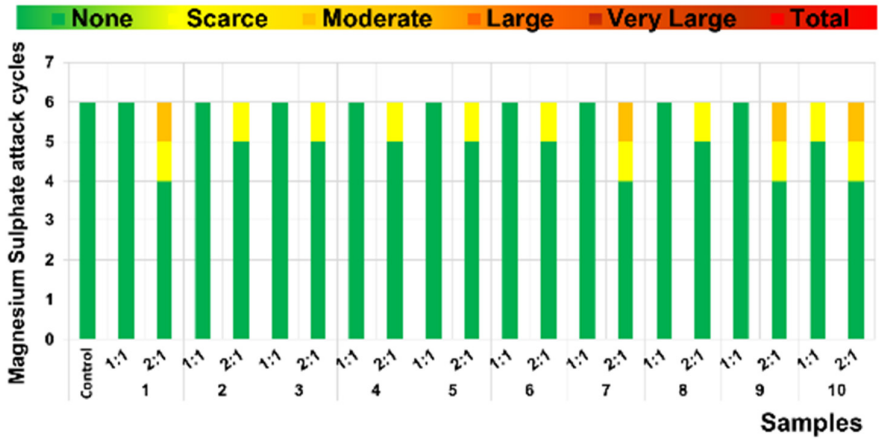

Figure 14. Degrees of alteration in samples following cycles of sulfate attack.

3.4. Leaching Studies

The measurements of leachates from the mining tailings were conducted according to Mexican regulations for the PECT extract test (NOM-053-SEMARNAT-1993). As observed in the previous study, lead (Pb) and arsenic (As) were released and quantified, as shown in Figure 15. The allowable maximum limit (AML) of Pb, as per NOM-052-SEMARNAT-2005 [53], was exceeded in all samples, as evidenced in Figure 15a. The release of As only exceeded the limits in samples 4 and 9 (Figure 15b).

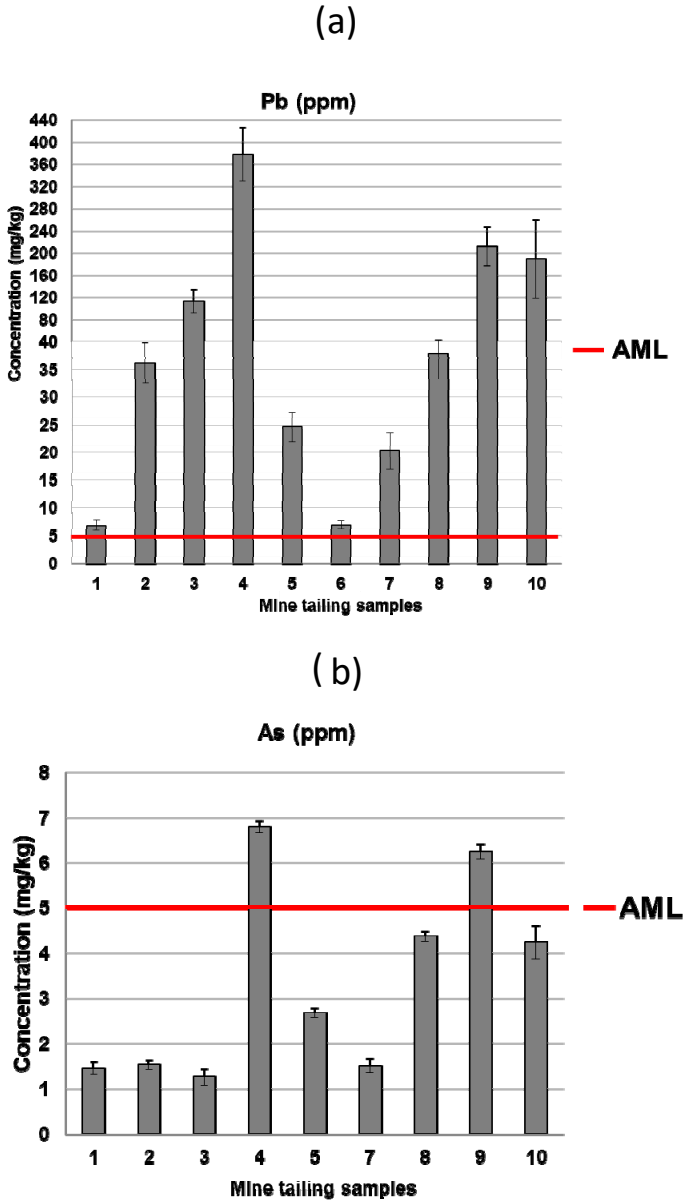

Figure 15. Leachate concentration of potentially toxic components in the mine tailings samples (**a**) Pb and (**b**) As (extraction test method NOM-053-SEMARNAT-1993) and allowable maximum limit (AML) values for hazardous waste disposal (NOM-052-SEMARNAT-2005).

According to the results of the predominant phases present in the mine tailings and also in the hardened mortars (e.g., microcline, biotite, or chalcopyrite), it can be deduced that the toxic Pb and As are mostly physically retained in the mortar matrix in the same

chemical form as in the source tailings. As discussed before, As and Pb appeared to be associated in some EDS spots, and weak X-ray diffraction peaks ascribed to the presence of lead-bearing arsenate compounds were identified. However, these findings were proven only in some samples and it is necessary to notice that the relatively low level of concentration of these elements precludes an undisputed speciation of these components by techniques such as X-ray diffraction or FTIR. According to the previous literature, to explain, besides the physical encapsulation, how potentially toxic elements would interact with the stabilizing matrix from a chemical point of view, two stages can be identified [54]: (i) interaction with the hydroxides present due to the free portlandite in the lime mortar, and (ii) the insolubility of the hydroxides of toxic metals, especially at high tailings doses. The pH and conductivity values of the different washings from the tank test were determined [1,14,55] (Figures 16 and 17), confirming that these conditions were prone to forming immobilized and not easily leachable chemical compounds. Additionally, as previously discussed, there was a decrease in the porosity of the monolithic matrix, contributing to the physical encapsulation.

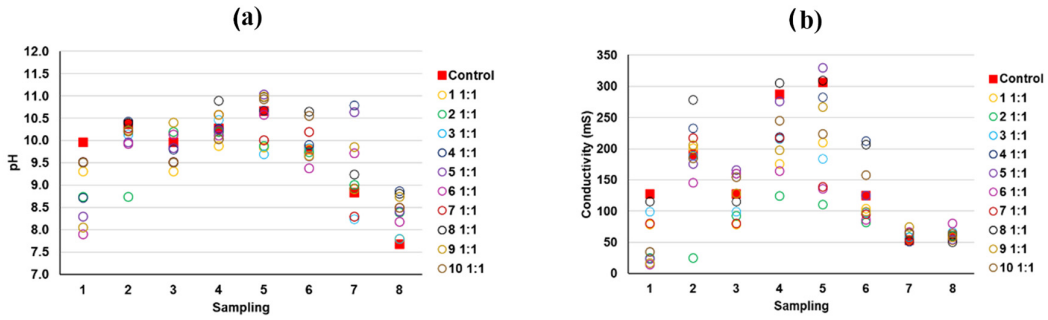

Figure 16. (**a**) pH and (**b**) conductivity of the leachates from the tank test (samples with 1:1 ratios of mine tailings/lime).

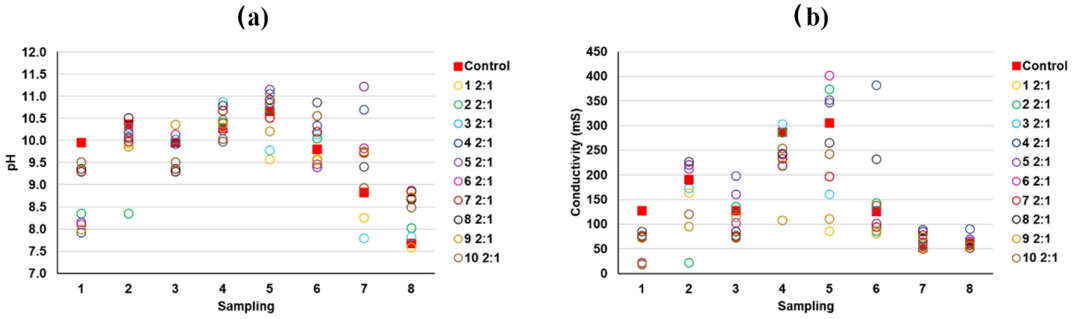

Figure 17. (**a**) pH and (**b**) conductivity of the leachates from the tank test (samples with 2:1 ratios of mine tailings/lime).

The experimental results corroborated the strong stability and limited solubility of the matrix formed by the modified lime mortar, ensuring the effective solidification/stabilization of Pb, the most prominent toxic metal in the tailings. Considering these outcomes related to metal release, along with the physical and chemical characteristics of the samples in their hardened state, the inclusion of tailings up to a 2:1 ratio, despite their diminished mechanical strength, can be proposed. Furthermore, it is evident from the presented data that the monolithic samples obtained using the proposed S/S method in this article can be used to encapsulate these residues in tailings dams, preventing migration to the surrounding population, as discussed in the work of Gonzalez, 2023 [32], thus reducing the health and environmental risks for the nearby population over time.

4. Conclusions

The use of a modified lime mortar as a binder for the stabilization/solidification of mine tailings presents a promising solution for immobilizing potentially toxic elements found in these waste materials. The results demonstrated the effectiveness of the modified lime mortar in avoiding the mobility of toxic elements in mining tailings. The 1:1 tailings waste/air lime ratio samples showed better mechanical strengths than (2:1) samples, with a more intense pozzolanic reaction. The (2:1) samples reflected a decrease in porosity due to the higher tailings density.

The joint EDS and XRD studies revealed the association of Fe with S in the form of pyrites. The strong association of Si, Al, and K was also observed, corresponding to the prominent presence of microcline ($KAlSi_3O_8$).

The encapsulation of mine tailings generated materials that satisfactorily withstood the freeze–thaw cycles without significant damage for up to 10 consecutive cycles. The resistance to sulfate attack in samples treated in magnesium sulfate solution showed the detrimental effect of compounds such as ettringite, formed by a reaction between C-A-H, portlandite, and sulfate ions. However, the samples endured up to four cycles without evident deterioration.

Characterization of the leachates showed that all the mine tailings exceeded the permissible Pb release limit, while two of them also exceeded the As threshold. The modified lime mortar allowed a very effective encapsulation of the toxic components, avoiding the release capacity of these compounds, which were completely absent in the leachates. In addition to the physical encapsulation, the strongly alkaline pH of the lime mortars aided the precipitation of insoluble hydroxides of both elements.

The advantages of employing lime mortar as a treatment method for mine tailings have thus been proven. Additionally, considering its cost-effectiveness, widespread availability, low CO_2 footprint, and ease of use, the application of modified lime mortar for the treatment of mine tailings can be recommended as a sustainable solution to mitigate the environmental impacts of mining activities.

Since mine tailings exhibited good compatibility with the modified lime mortar, this treatment method could be utilized to apply an in situ coating to tailings dams with the aim of mitigating the migration of such waste towards nearby communities, thus reducing the risk of potential health impacts.

Supplementary Materials: The following supporting information can be downloaded at https://www.mdpi.com/article/10.3390/su16062320/s1, Figure S1. FTIR spectrum of the control sample. Identification of the main absorption bands. Figure S2. FTIR spectra of the tested samples. Figure S3. FTIR spectra of the tested samples (zoom at 1000 cm^{-1}). Figure S4. TG-DSC curves of the tested samples. Figure S5. EDS element composition results of spots of the needle-like structures in the sample 5 (1:1). Figure S6. EDS element composition results of spots of the needle-like structures in the sample 5 (1:1). Figure S7. EDS element composition results of spots of the needle-like structures in the sample 5 (1:1).

Author Contributions: Conceptualization, J.I.A., Í.N.-B., J.M.F. and J.F.G.-S.; methodology, J.F.G.-S., Í.N.-B. and J.I.A.; validation, J.F.G.-S., G.F.-V. and A.U.L.J.; formal analysis, J.F.G.-S. and Í.N.-B.; investigation, J.F.G.-S., Í.N.-B. and J.I.A.; resources, G.F.-V. and A.U.L.J.; data curation, A.U.L.J. and Í.N.-B.; writing—original draft preparation, J.F.G.-S.; writing—review and editing, J.I.A., J.M.F., J.F.G.-S. and G.F.-V.; visualization, J.I.A. and J.M.F.; supervision, J.I.A. and Í.N.-B.; project administration, J.F.G.-S. and G.F.-V.; funding acquisition, J.F.G.-S., G.F.-V., Í.N.-B. and J.I.A. All authors have read and agreed to the published version of the manuscript.

Funding: The first author thanks Dirección General de Asuntos del Personal Academico (DGAPA), by Universidad Nacional Autónoma de México (UNAM), for the postdoctoral grant. This research was funded by the Spanish Ministerio de Ciencia e Innovación MICINN, grant numbers PID2020-119975RB-100 LIMORTHER, Terra Cycle TED2021-129705-C33.

Institutional Review Board Statement: Not applicable.

Informed Consent Statement: Not applicable.

Data Availability Statement: The data presented in this study are available on request from the corresponding author.

Acknowledgments: The authors thank the technical support provided by Ana E. Silva, Mario A. Minor, Ana Paola Chango, Elsy Gabriela de Santiago, and Cristina Luzuriaga.

Conflicts of Interest: The authors declare no conflicts of interest.

References

1. Loredo-Portales, R.; Bustamante-Arce, J.; González-Villa, H.N.; Moreno-Rodríguez, V.; Del Rio-Salas, R.; Molina-Freaner, F.; González-Méndez, B.; Archundia-Peralta, D. Mobility and Accessibility of Zn, Pb, and As in Abandoned Mine Tailings of Northwestern Mexico. *Environ. Sci. Pollut. Res.* **2020**, *27*, 26605–26620. https://doi.org/10.1007/s11356-020-09051-1.
2. Corrales-Pérez, D.; Romero, F.M. Evaluacion de La Peligrosidad de Jales de Zonas Mineras de Nicaragua y Mexico y Alternativas de Solucion. *Bol. Soc. Geol. Mex.* **2013**, *65*, 427–446. https://doi.org/10.18268/BSGM2013v65n3a1.
3. Xiaolong, Z.; Shiyu, Z.; Hui, L.; Yingliang, Z. Disposal of Mine Tailings via Geopolymerization. *J. Clean. Prod.* **2020**, *284*, 124756. https://doi.org/10.1016/j.jclepro.2020.124756.
4. Punia, A.; Singh, S.K. Contamination of Water Resources in the Mining Region. In *Contamination of Water: Health Risk Assessment and Treatment Strategies*; Ahamad, A., Siddiqui, S.I., Singh, P., Eds.; Academic Press: Cambridge, MA, USA; Elsevier: Amsterdam, The Netherlands, 2021.
5. López-Ramírez, C.; Cuevas-Cardona, C. Mining Waste and the Pachuca River. *Hist. Ambient. Latinoam. Caribeña* **2022**, *12*, 193–213. https://doi.org/10.32991/2237-2717.2022v12i3.p193-213.
6. Santana, C.S.; Montalván Olivares, D.M.; Silva, V.H.C.; Luzardo, F.H.M.; Velasco, F.G.; de Jesus, R.M. Assessment of Water Resources Pollution Associated with Mining Activity in a Semi-Arid Region. *J. Environ. Manag.* **2020**, *273*, 111148. https://doi.org/10.1016/j.jenvman.2020.111148.
7. Okewale, I.A.; Grobler, H. Assessment of heavy metals in tailings and their implications on human health. *Geosyst. Geoenviron.* **2023**, *2*, 100203. https://doi.org/10.1016/j.geogeo.2023.100203.
8. García, I.C.G.; Villagómez, G.F.; Pérez, A.M.; Torres, L.A.B.; García, A.G. Policy Proposal for Metals Speciation in Tailings Contaminated Soils: A Case Study in Chihuahua, Mexico. *J. Mex. Chem. Soc.* **2017**, *61*, 14–22.
9. Mendoza-Benítes, I.; de la Rosa-Álbarez, M.G.; Cruz-Jiménez, G. Identificación de Especies Vegetales Relacionadas Con Jales Mineros Del Distrito Minero de Guanajuato. *Biológicas* **2008**, *10*, 94–99.
10. Cardenas, J. The Mining Industry in Mexico: The Dispossession of the Nation. *Cuest. Const.* **2013**, *28*, 35–74. https://doi.org/10.1016/s1405-9193(13)71275-7.
11. Tetreault, D. Social Environmental Mining Conflicts in Mexico. *Lat. Am. Perspect.* **2015**, *42*, 48–66. https://doi.org/10.1177/0022429415585112.
12. Méndez, M.; Armienta, M.A. Arsenic Phase Distribution in Zimapán Mine Tailings, Mexico. *Geofísica Int.* **2003**, *42*, 131–140. https://doi.org/10.22201/igeof.00167169p.2003.42.1.366.
13. Kossoff, D.; Dubbin, W.E.; Alfredsson, M.; Edwards, S.J.; Macklin, M.G.; Hudson-Edwards, K.A. Mine Tailings Dams: Characteristics, Failure, Environmental Impacts, and Remediation. *Appl. Geochem.* **2014**, *51*, 229–245.
14. Tian, Q.; Bai, Y.; Pan, Y.; Chen, C.; Yao, S.; Sasaki, K.; Zhang, H. Application of Geopolymer in Stabilization/Solidification of Hazardous Pollutants: A Review. *Molecules* **2022**, *27*, *4570*. https://doi.org/10.3390/molecules27144570.
15. Li, W.; Ni, P.; Yi, Y. Comparison of Reactive Magnesia, Quick Lime, and Ordinary Portland Cement for Stabilization/Solidification of Heavy Metal-Contaminated Soils. *Sci. Total Environ.* **2019**, *671*, 741–753. https://doi.org/10.1016/j.scitotenv.2019.03.270.
16. Lasheras-Zubiate, M.; Navarro-Blasco, I.; Fernández, J.M.; Álvarez, J.I.; Encapsulation, Solid-Phases Identification and Leaching of Toxic Metals in Cement Systems Modified by Natural Biodegradable Polymers. *J. Hazard. Mater.* **2012**, *233–234*, 7–17. https://doi.org/10.1016/j.jhazmat.2012.06.028.
17. Kundu, S.; Gupta, A.K. Immobilization and Leaching Characteristics of Arsenic from Cement and/or Lime Solidified/Stabilized Spent Adsorbent Containing Arsenic. *J. Hazard. Mater.* **2008**, *153*, 434–443. https://doi.org/10.1016/j.jhazmat.2007.08.073.
18. Groot, C.; Hughes, J.J. RILEM TC 203-RHM : Repair Mortars for Historic Masonry : Performance Requirements for Renders and Plasters RILEM TECHNICAL COMMITTEE RILEM TC 203-RHM : Repair Mortars for Historic Masonry. *Mater. Struct.* **2012**, *45*, 1277–1285. https://doi.org/10.1617/s11527-012-9916-0.
19. Li, G.; Li, H.; Li, Y.; Chen, X.; Li, X.; Wang, L.; Zhang, W.; Zhou, Y. Stabilization/Solidification of Heavy Metals and PHe Contaminated Soil with β-Cyclodextrin Modified Biochar (β-CD-BC) and Portland Cement. *Int. J. Environ. Res. Public Health* **2022**, *19*, 1060. https://doi.org/10.3390/ijerph19031060.
20. Li, J. shan; Chen, L.; Zhan, B.; Wang, L.; Poon, C.S.; Tsang, D.C.W. Sustainable Stabilization/Solidification of Arsenic-Containing Soil by Blast Slag and Cement Blends. *Chemosphere* **2021**, *271*, 129868. https://doi.org/10.1016/j.chemosphere.2021.129868.
21. Chen, L.; Nakamura, K.; Hama, T. Review on Stabilization/Solidification Methods and Mechanism of Heavy Metals Based on OPC-Based Binders. *J. Environ. Manag.* **2023**, *332*, 117362. https://doi.org/10.1016/J.JENVMAN.2023.117362.
22. Conner, J.R.; Hoeffner, S.L. A Critical Review of Stabilization/Solidification Technology. *Crit. Rev. Environ. Sci. Technol.* **1998**, *28*, 397–462. https://doi.org/10.1080/10643389891254250.

23. Van Jaarsveld, J.G.S.; Van Deventer, J.S.J.; Schwartzman, A. The Potential Use of Geopolymeric Materials to Immobilise Toxic Metals: Part II. Material and Leaching Characteristics. *Miner. Eng.* **1999**, *12*, 75–91. https://doi.org/10.1016/S0892-6875(98)00121-6.
24. Fragata, A.; Veiga, R. Air Lime Mortars: The Influence of Calcareous Aggregate and Filler Addition. In *Proceedings of the Materials Science Forum*; Trans Tech Publications Ltd.: Stafa-Zurich, Switzerland, 2010; Volume 636–637, pp. 1280–1285.
25. Westgate, P.; Ball, R.J.; Paine, K. Olivine as a Reactive Aggregate in Lime Mortars. *Constr. Build. Mater.* **2019**, *195*, 115–126. https://doi.org/10.1016/J.CONBUILDMAT.2018.11.062.
26. García-González, J.; Faria, P.; Pereira, A.S.; Lemos, P.C.; Juan-Valdés, A. A Sustainable Production of Natural Hydraulic Lime Mortars through Bio-Amendment. *Constr. Build. Mater.* **2022**, *340*, 127812. https://doi.org/10.1016/J.CONBUILDMAT.2022.127812.
27. Pinto, P.X.; Al-Abed, S.R.; Barth, E.; Loftspring, C.; Voit, J.; Clark, P.; Ioannides, A.M. Environmental Impact of the Use of Contaminated Sediments as Partial Replacement of the Aggregate Used in Road Construction. *J. Hazard. Mater.* **2011**, *189*, 546–555. https://doi.org/10.1016/J.JHAZMAT.2011.02.074.
28. Choi, W.H.; Lee, S.R.; Park, J.Y. Cement Based Solidification/Stabilization of Arsenic-Contaminated Mine Tailings. *Waste Manag.* **2009**, *29*, 1766–1771. https://doi.org/10.1016/j.wasman.2008.11.008.
29. Ghafari, E.; Costa, H.; Júlio, E.; Portugal, A.; Durães, L. The Effect of Nanosilica Addition on Flowability, Strength and Transport Properties of Ultra High Performance Concrete. *Mater. Des.* **2014**, *59*, 1–9. https://doi.org/10.1016/j.matdes.2014.02.051.
30. Malathy, R.; Shanmugam, R.; Chung, I.M.; Kim, S.H.; Prabakaran, M. Mechanical and Microstructural Properties of Composite Mortars with Lime, Silica Fume and Rice Husk Ash. *Processes* **2022**, *10*, 1424. https://doi.org/10.3390/pr10071424.
31. Gleize, P.J.P.; Müller, A.; Roman, H.R. Microstructural Investigation of a Silica Fume-Cement-Lime Mortar. *Cem. Concr. Compos.* **2003**, *25*, 171–175. https://doi.org/10.1016/S0958-9465(02)00006-9.
32. González-Sánchez, J.F.; Mendoza-Lara, O.O.; Romero-Hernández, J.L.; Fernández-Villagómez, G. Evaluation of the Danger of a Tailings Pile Belonging to an Active Mine through Its Characterization and a Dispersion Model. *Environ. Monit. Assess.* **2023**, *195*. https://doi.org/10.1007/S10661-023-11475-4.
33. Marín-García, H.J.; Escudero-Carcía, R.; Cortés-Penagos, C.; Cholico-González, D.F. Chemical Characterization and Quantification of Metallic Gold from Copper Tailings in the Western Region of Mexico. *MRS Adv.* **2022**, *7*, 1072–1077. https://doi.org/10.1557/s43580-022-00437-6.
34. Carmignano, O.R.; Vieira, S.S.; Teixeira, A.P.C.; Lameiras, F.S.; Brandão, P.R.G.; Lago, R.M. Iron Ore Tailings: Characterization and Applications. *J. Braz. Chem. Soc.* **2021**, *32*, 1875–1911. https://doi.org/10.21577/0103-5053.20210100.
35. Nalon, G.H.; Alves, M.A.; Pedroti, L.G.; Lopes Ribeiro, J.C.; Hilarino Fernandes, W.E.; Silva de Oliveira, D. Compressive strength, dynamic, and static modulus of cement-lime laying mortars obtained from samples of various geometries. *J. Build. Eng.* **2021**, *44*, 102626. https://doi.org/10.1016/j.jobe.2021.102626.
36. Su-Cadirci, T.B.; Calabria-Holley, J.; Ince, C.; Ball, R.J. Freeze-Thaw Resistance of Pozzolanic Hydrated Lime Mortars. *Constr. Build. Mater.* **2023**, *394*, 131993. https://doi.org/10.1016/J.CONBUILDMAT.2023.131993.
37. Secretaría de Economía. *NMX-C-159-ONCCE-2016*; Industria de La Construcción—Concreto—Elaboración y Curado de Especímenes de Ensayo. Organismo Nacional de Normalización y Certificación de la Construcción y Edificación, S.C.: Mexico City, Mexico, 2016; pp. 1–15.
38. *European Committee for Standardization UNE-EN 196-1*; Methods of Testing Cement. Part 1: Determination of Strength. CEN: Brussels, Belgium, 2018.
39. *European Committee for Standardization UNE-EN 1015-3:2000*. Methods of Test for Mortar for Masonry—Part 3: Determination of Consistence of Fresh Mortar (by Flow Table). CEN: Brussels, Belgium, 2000.
40. *ASTM C39/C39M*; Standard Test Method for Compressive Strength of Cylindrical Concrete Specimens. American Society for Testing and Materials: West Conshohocken, PA, USA, 2001; pp. 1–8.
41. Corona Sánchez, J.E.; González Chávez, M.d.C.A.; Carrillo González, R.; Scheckel, K.; Tapia Maruri, D.; García Cue, J.L. Metal(Loid) Bioaccessibility of Atmospheric Particulate Matter from Mine Tailings at Zimapan, Mexico. *Environ. Sci. Pollut. Res.* **2021**, *28*, 19458–19472. https://doi.org/10.1007/s11356-020-11887-6.
42. Secretaría de Medio Ambiente y Recursos Naturales (SEMARNAT). *Norma Oficial Mexicana NOM-053-SEMARNAT-1993*; Diario Oficial de la Federación: Mexico City, Mexico, 1993.
43. European Committee for Standardization EA NEN 7375. *Leaching Characteristics of Moulded or Monolithic Building and Waste Materials. Determination of Leaching of Inorganic Components with the Diffusion Test*. NEN: Delft,The Netherlands, 2004.
44. Zarzuela, R.; Luna, M.; Carrascosa, L.M.; Yeste, M.P.; Garcia-Lodeiro, I.; Blanco-Varela, M.T.; Cauqui, M.A.; Rodríguez-Izquierdo, J.M.; Mosquera, M.J. Producing C-S-H Gel by Reaction between Silica Oligomers and Portlandite: A Promising Approach to Repair Cementitious Materials. *Cem. Concr. Res.* **2020**, *130*, 106008. https://doi.org/10.1016/J.CEMCONRES.2020.106008.
45. Grilo, J.; Silva, A.S.; Faria, P.; Gameiro, A.; Veiga, R.; Velosa, A. Mechanical and Mineralogical Properties of Natural Hydraulic Lime-Metakaolin Mortars in Different Curing Conditions. *Constr. Build. Mater.* **2014**, *51*, 287–294. https://doi.org/10.1016/j.conbuildmat.2013.10.045.
46. Lewis, R.; Fidjestøl, P. *Microsilica as an Addition*; 5th ed.; Elsevier Ltd.: Amsterdam, The Netherlands, 2019; ISBN 9780081007730.
47. Villca, A.R.; Soriano, L.; Font, A.; Tashima, M.M.; Monzó, J.; Borrachero, M.V.; Payá, J. Lime/pozzolan/geopolymer systems: Performance in pastes and mortars. *Constr. Build. Mat.* **2021**, 276, 122208. https://doi.org/10.1016/j.conbuildmat.2020.122208.

48. Pavía, S.; Toomey, B. Influence of the Aggregate Quality on the Physical Properties of Natural Feebly-Hydraulic Lime Mortars. *Mater. Struct. Constr.* **2008**, *41*, 559–569. https://doi.org/10.1617/s11527-007-9267-4.
49. Ceniceros-Gómez, A.E.; Macías-Macías, K.Y.; de la Cruz-Moreno, J.E.; Gutiérrez-Ruiz, M.E.; Martínez-Jardines, L.G. Characterization of Mining Tailings in México for the Possible Recovery of Strategic Elements. *J. S. Am. Earth Sci.* **2018**, *88*, 72–79. https://doi.org/10.1016/j.jsames.2018.08.013.
50. Al-Akhras, N.M. Durability of Metakaolin Concrete to Sulfate Attack. *Cem. Concr. Res.* **2006**, *36*, 1727–1734. https://doi.org/10.1016/J.CEMCONRES.2006.03.026.
51. Aziez, M.N.; Bezzar, A. Magnesium Sulphate Attacks on Mortars—Influence of Temperature, Type of Sand and Type of Cement. *J. Eng. Sci. Technol. Rev.* **2017**, *10*, 41–50. https://doi.org/10.25103/jestr.101.07.
52. De Souza, D.J.; Sanchez, L.F.M.; Filho, J.H.; Medeiros, M.H.F. Development of a durability indicator to forecast the efficiency of preventive measures against external sulphate attack. *Cem. Concr. Compos.* **2024**, *145*, 105349. https://doi.org/10.1016/j.cemconcomp.2023.105349.
53. Secretaría de Medio Ambiente y Recursos Naturales (SEMARNAT). *Norma Oficial Mexicana NOM-052-SEMARNAT-2005*; Diario Oficial de la Federación, Mexico City, Mexico, 2005.
54. Todaro, F.; Colangelo, F.; De Gisi, S.; Farina, I.; Ferone, C.; Labianca, C.; Petrella, A.; Cioffi, R.; Notarnicola, M. Recycling of Contaminated Marine Sediment and Industrial By-Products through Combined Stabilization/Solidification and Granulation Treatment. *Materials* **2023**, *16*, 2399. https://doi.org/10.3390/MA16062399.
55. Long, W.J.; Lin, C.; Ye, T.H.; Dong, B.; Xing, F. Stabilization/Solidification of Hazardous Lead Glass by Geopolymers. *Constr. Build. Mater.* **2021**, *294*, 123574. https://doi.org/10.1016/j.conbuildmat.2021.123574.